

ASTROPHYSICAL S-FACTOR OF ${}^6\text{Li}(p,\gamma){}^7\text{Be}$ REACTION FROM EXPERIMENTAL DATA USING DIFFERENT METHODS

N. Burtebayev¹, A. Amar², S.B. Dubovichenko³, S.B. Sakuta⁴, S.V. Artemov⁵,
Zh. Kerimkulov¹

¹*Institute of Nuclear Physics of National Nuclear Center, Almaty, Kazakhstan*

²*Kazakh National University, Almaty, Kazakhstan*

³*V. G. Fesenkov Astrophysical Institute of NSRTC NSA of RK, Almaty, Kazakhstan*

⁴*Russian Research Center "Kurchatov institute", Moscow, Russia*

⁵*Institute of Nuclear Physics, Tashkent, Uzbekistan*

New measurements of the ${}^6\text{Li}(p,\gamma){}^7\text{Be}$ reaction γ -ray angular distributions have been done at beam energies of $E_{p, \text{lab.}} = 387, 690, 984$ and 1283 keV for the γ -ray transitions to the ground and first excited ($1/2^-$, 429 keV) states in ${}^7\text{Be}$. Our calculations of the cross section of the ${}^6\text{Li}(p,\gamma){}^7\text{Be}$ reaction was carried within the framework of the direct capture in the potential model using Fresco program. We extracted both of spectroscopic factors of ${}^7\text{Be}$ and astro S-factor ${}^6\text{Li}+p \rightarrow {}^7\text{Be}+\gamma$ from experimental data using two different methods.

Introduction

The OMPs are widely employed to generate the distorted waves used to analyze the cross section of many reactions, and these analyses have proved to be powerful tool to extract nuclear structure information [1]. Reactions at astrophysical energies are complicated by the fact that the matter-interaction energy in stars is very low, ranging between a few tenths of a keV unit and a few tens of keV units. With a few exceptions, it is next to impossible under laboratory conditions to measure directly, at such energies, nuclear-reaction cross sections, which are necessary for astrophysical calculations. Usually, cross sections are measured at higher energies, whereupon the results are extrapolated to the energy region of interest for nuclear astrophysics. As a rule, however, the measurements actually performed cover only the region of rather high energies from about 0.2 to 1 MeV. In view of this, an extrapolation of such experimental data to the astrophysical region is not always justified. As a result, only theoretical predictions can compensate in many cases for missing experimental information about the properties of astrophysical thermonuclear reactions. Under such conditions, resort to realistic models that are rather simple in practical applications, such as the potential cluster model (PCM), seems quite justified. Usually, the results of calculations performed on the basis of model concepts are contrasted against available low-energy experimental data, and approaches leading to the best agreement with these data are selected by using the results of this comparison. After that, calculations in the region of astrophysical energies are performed within the chosen conceptual framework. One can consider the results obtained in this way (for example, those concerning astrophysical S factors) as more realistic estimates of respective quantities than the extrapolation of experimental data, since the theoretical models used have, as a rule, quite a sound microscopic basis [2]. Radiative capture of nucleons at energies of astrophysics interest is one of the most important processes for nucleosynthesis. The nucleon capture can occur either by a compound nucleus reaction or by direct process. The compound reaction cross sections are usually small, especially for light nuclei. The direct capture proceeds either via the formation of a single-particle resonance or non-resonant capture process. Unlike ${}^7\text{Li}$ and ${}^6\text{Li}$ to be formed at very low level in Big Bang nucleosynthesis, with abundance ratio $\text{Li}/\text{H} = 10^{-14}$. Whereas most elements are produced by stellar nucleosynthesis, lithium is mainly destroyed in stellar interiors by thermonuclear reactions with protons. In fact, ${}^6\text{Li}$ is rapidly consumed at stellar temperature 2×10^6 K. The low energy capture reaction ${}^6\text{Li}(p,\gamma){}^7\text{Be}$ plays an important role in the consumption of ${}^6\text{Li}$ and formation of ${}^7\text{Be}$ [3].

The S-factor of this reaction is dominated by captures to the ground state and first excited state of ${}^7\text{Be}$. However, the number of studies devoted to measuring the total cross section for this reaction and to experimentally determining its astrophysical S factor in the region of low energies is comparatively small [4]. The ${}^6\text{Li}(p,\gamma){}^7\text{Be}$ reaction has been experimentally studied by Switkowski *et al.* [5] at low energies down to 200keV. A theoretical extrapolation has been performed by Barker [6] within potential model, based on simultaneous fit of ${}^6\text{Li}(n,\gamma){}^7\text{Li}$ and ${}^6\text{Li}(p,\gamma){}^7\text{Be}$ cross sections. K. Arai *et al.* [7] used a four cluster microscopic model to investigate low-energy ${}^6\text{Li}+p$ and ${}^6\text{Li}+n$ reactions.

The ${}^6\text{Li}(p,\gamma){}^7\text{Be}$ reaction S-factor is in [7] good agreement with the available experimental data. Knowledge of the rate of change of the S factor with energy at very low energies is needed to perform a reliable extrapolation. Although this is frequently determined by the use of a direct capture-model calculation, there are cases when this does not suffice. Low-energy resonances or sub-threshold states can affect the extrapolation. In [8] the results of a measurement of the slope of the astrophysical S factor for the ${}^6\text{Li}(p,\gamma){}^7\text{Be}$ reaction are reported, and a new mechanism is introduced to explain the observed slope. Cecil *et al.* [9] measured the branching ratio of ${}^6\text{Li}(p,\gamma_0){}^7\text{Be}$ and ${}^6\text{Li}(p,\gamma_1){}^7\text{Be}$ with respect to ${}^6\text{Li}(p,\alpha){}^3\text{He}$ from 45 to 170 keV and deduced the S factors for ${}^6\text{Li}(p,\gamma_0){}^7\text{Be}$ and ${}^6\text{Li}(p,\gamma_1){}^7\text{Be}$ as a function of energy. Their results gave a positive slope for the S factor. Switkowski *et al.* [5] measured the ${}^6\text{Li}(p,\gamma){}^7\text{Be}$ cross section from 160 to 1150 keV. Their data points are all at energies above the present data set and show an S factor that increases with increasing energy. Barker's analysis [6] of the data of Switkowski *et al.* does have a negative S -factor slope for ${}^6\text{Li}(p,\gamma_0){}^7\text{Be}$ and ${}^6\text{Li}(p,\gamma_1){}^7\text{Be}$ at energies below the range of the data. The present measurements were undertaken to examine this discrepancy in the previous measurements of Cecil *et al.* and Switkowski *et al.*

The purpose of this work is to extract the spectroscopic factors of ${}^7\text{Be}$ from the ${}^6\text{Li}(p,\gamma){}^7\text{Be}$ reaction and then use these values to extract astro S-factor ${}^6\text{Li}+p\rightarrow{}^7\text{Be}+\gamma$.

Experimental Data

a) ${}^6\text{Li}(p,p){}^6\text{Li}$

Measurements of elastic scattering of protons on ${}^6\text{Li}$ nuclei at low energy region were carried out with using the extracted beam from UKP-2-1 accelerator of the Institute of Nuclear Physics (National Nuclear Center, Republic of Kazakhstan, Almaty, Kazakhstan) in the angular range 30-170°. The proton energy varied in the range 400 – 1150 keV. The beam intensity was 50 – 150 nA. Scattered particles were detected using surface-barrier silicon counters. Experiment set up was mentioned in [10].

b) ${}^6\text{Li}(p,\gamma){}^7\text{Be}$

In experiment for determination of cross-sections of the ${}^6\text{Li}(p,\gamma){}^7\text{Be}$ reaction, it was used special manufactured chamber with indium vacuum seals, systems of fine adjustment and visual control of the form of proton beam and its position on the target during all measurements, with the possibility of precise placement of the target exactly into the chamber center and of its additional equipment by nitrogen trap and additional magneto-discharge pump. The new reaction chamber was connected to the output flange of the central scattering chamber, completed by turbo-molecular and magneto-discharge pumps and by the system of nitrogen traps. The typical pressure in the reaction chamber was $1.5\cdot 10^{-6}$ mm Hg, and the experimental error, stipulated by the formation of carbon deposit on the target during the measurement, was negligible. The measurements of angular distributions of gamma-quanta from the ${}^6\text{Li}(p,\gamma){}^7\text{Be}$ for transitions were for the ground state and first excited state (429 keV) of the ${}^7\text{Be}$ at energies of incident protons of 387, 690, 984 and 1283 keV. Currents of the protons beam, incident upon targets, were equal to (5-8) μA . During the

measurement of the integral current the collected charge was from 0.05 to 0.25 Coulomb. Targets were placed in the chamber for the study of (p, γ) reactions.

In order to prevent the overload of the electronics, caused by the powerful background line with the energy of $E_\gamma=478$ keV, connected with progresses, ${}^7\text{Li} (p, p\gamma){}^7\text{Li}$ and ${}^7\text{Be}\rightarrow{}^7\text{Li}^*+\beta^++\nu\rightarrow{}^7\text{Li}+478$ keV, between the detector and the reaction region there was put the flat lead plate of the 1 cm-thickness. Besides, the intensity of the line with $E_\gamma=478$ keV decreases by a factor of about 5, whereas the intensity of lines from the ${}^6\text{Li}(p,\gamma){}^7\text{Be}$ reaction (with $E_\gamma=6000$ keV) decreases only by several per cent. Fig.1. is an example of the γ -spectrum, obtained at $E_{p,\text{lab}}=984$ keV, $\theta_{\gamma,\text{lab}}=0^\circ$. In figure there are well seen background lines, 1461 keV (${}^{40}\text{K}$), and the annihilation line with $E_\gamma=511$ keV. Well-known energies of γ -transitions for these lines allowed to control the energy calibration. Peaks of the total absorption and peaks of unitary and double leakages for γ -transitions onto the ground and the first excited state of the ${}^7\text{Be}$ shown in Figure 1, with the use of the HpGe – detector (GEM20P) of the 111cm^3 –volume, placed in 6 cm from the reaction region.

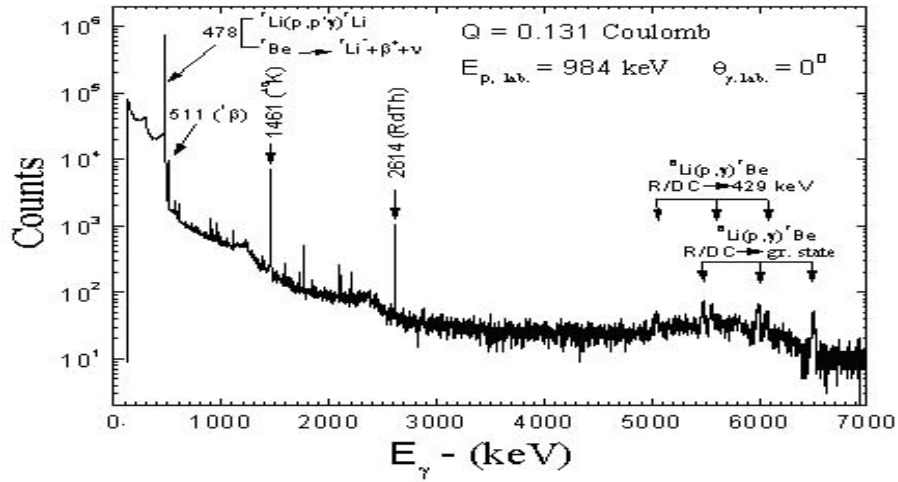


Fig. 1. An example of the γ -spectrum of the ${}^6\text{Li}(p,\gamma){}^7\text{Be}$ reaction

Results and Discussions

a) Phenomenological Elastic Scattering of protons on ${}^6\text{Li}$

The analysis of protons data, carried out at wide energy range, had shown that for ${}^6\text{Li}$ nuclei, the most suitable parameters values are $r_0=1.05\text{fm}$, $r_c=1.3\text{fm}$, $r_D=1.923\text{fm}$, $a_s=0.20\text{fm}$ and $r_s=1.20$ fm, complete analysis have been mentioned at [11].

Table 1. The phenomenological optical parameters for protons scattering on Lithium nuclei

| E_p , MeV | V_0 , MeV | r_0 , fm | a_0 , fm | W_D , MeV | r_D , fm | a_D , fm | V_S , MeV | r_s , fm | a_s , fm | J_R , MeVfm ³ | J_w , MeVfm ³ |
|-------------|-------------|------------|------------|-------------|------------|------------|-------------|------------|------------|----------------------------|----------------------------|
| 0.746 | 59 | 1.05 | 0.85 | 0.300 | 1.923 | 0.575 | 9.30 | 1.077 | 0.66 | 490 | 20.47 |
| 0.975 | 57.2 | 1.050 | 0.67 | 0.355 | 1.923 | 0.650 | 9.30 | 1.020 | 0.200 | 475 | 22.19 |
| 1.136 | 54 | 1.05 | 0.52 | 0.355 | 1.923 | 0.57 | 9.30 | 1.020 | 0.200 | 454 | 22.19 |

In the analogous approach with the use of measured on the elastic scattering there are determined parameters of the potential of protons scattering on ${}^6\text{Li}$ nuclei from the analysis of these data on the optical model. Obtained parameters of optical potentials of the interaction are presented in Table 1. The relations

between $V(W_D)$ versus E_p are linear. The strength parameters can be represented by: $V_0 = 56.10 - 0.61E_p$, $W_D = -0.66 + 0.46E_p$, respectively.

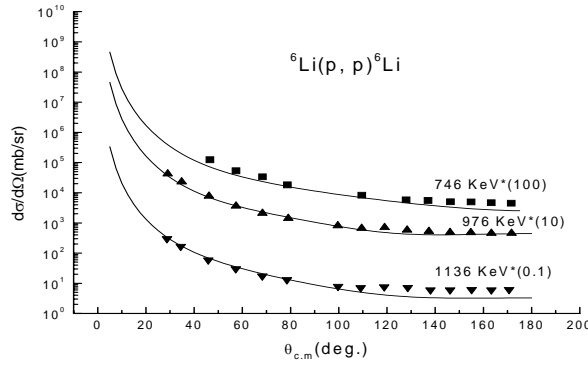


Fig. 2. The comparison between calculated and experimental angular distribution of protons scattered from ${}^6\text{Li}$ at low energies where dots represent experimental data and lines represent the calculated values

b) ${}^6\text{Li}(p,\gamma){}^7\text{Be}$ reaction at the low energies

For each angle the γ -detector was 6 cm from the beam spot on the target. The detector just as the calibration sources was placed to within 1 mm. The calibration source of ${}^{137}\text{Cs}$ ($E_\gamma = 661.66$ keV) was used to construct the dependence on γ -rays registration rate from the source detector distance. It was determined that at a distance of 6 cm the deviation on ± 1 mm results in a change of registration rate on 3.2%. So, the overall uncertainty of the absolute γ -detector photo-peak efficiency determination introduced by statistical uncertainty of γ -ray counts determination, dead time of the measuring electronics and inaccuracy of the γ -detector position was adopted 5.5% along the whole range of energies of registered γ -rays. The angular distributions of the ${}^6\text{Li}(p,\gamma){}^7\text{Be}$ reaction were fitted at four fixed energies from the energy region of $E_{p, \text{lab.}} = 387 - 1283$ keV by Legendre polynomials [12]:

$$W(\theta_\gamma) = 1 + \sum_k a_k Q_k P_k(\cos\theta) \quad (k = 1, 2, \dots), \quad (1)$$

where a_k are the expansion coefficients and Q_k are the attenuation coefficients, which take into account solid angle subtended by the γ -detector. In view of the limited number of angles, the fits were carried out by including only $k = 1$ and 2. The lower limits of Q_1 and Q_2 were calculated for the conditions of experiment within the point radioactive source approach by using the known dimensions of sensitive region of the γ -detector, the source-detector distances (D), and without taking lead plate located in front of the γ -detector into account. The lower limits of Q_1 and Q_2 were calculated for the conditions of experiment within the point radioactive source approach by using the known dimensions of sensitive region of the γ -detector, the source-detector distances (D), and without taking lead plate located in front of the γ -detector into account. In this connection according to Ref. [8], Q_i can be written:

$$Q_i = \frac{J_i}{J_0} \quad (i = 1, 2), \quad (2)$$

where $J_k = \sum_{i=0}^3 \int_{\theta_i}^{\theta_{i+1}} P_k(\cos \alpha) \cdot [1 - e^{-\mu(E_\gamma) \cdot l_{i+1}(\alpha)}] \cdot \sin \alpha \cdot d\alpha$, ($k = 0, 1, 2$), and $\mu(E_\gamma)$ is absorption coefficient.

First Method for S-factor calculation

Depending on our calculations [10, 11] for ${}^6\text{Li}(p, p){}^6\text{Li}$, we could calculate enhanced optical potential parameters at low energies. Spectroscopic factors have been extracted from our experimental data of the radiative reaction ${}^6\text{Li}(p, \gamma){}^7\text{Be}$. Our calculations of the cross section of the ${}^6\text{Li}(p, \gamma){}^7\text{Be}$ reaction was carried within the framework of the direct capture in the potential model using FRESKO Code. The calculation of the cross sections depended on OMPs and spectroscopic factors. For us it was cheerful results to obtain the values of cross section directly from our calculations depending on OMPs from the reaction ${}^6\text{Li}(p, p){}^6\text{Li}$. The relation between spectroscopic factors and optical potential parameters used was verified here very clear. As shown in fig. 3, when we fixed spectroscopic factors from [13], we obtained dot line.

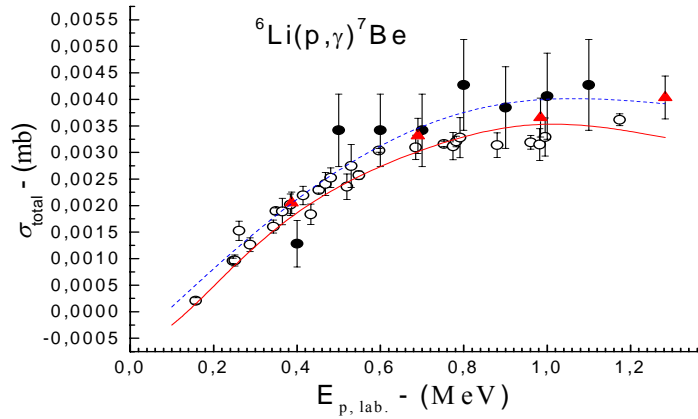


Fig. 3 total cross section of the reaction ${}^6\text{Li}(p, \gamma){}^7\text{Be}$. The experimental points are from [5] (open circles), [14] (closed circles) and our measurements as triangle. Solid line is calculated data depending on the OMPs from ${}^6\text{Li}(p, p){}^6\text{Li}$ in ref. [10,11] where dot line represents the calculations in case of OMPs taken from [15]

Table 2 Spectroscopic factors extracted for ${}^7\text{Be}$ from the radiative reaction ${}^6\text{Li}(p, \gamma){}^7\text{Be}$

| E(p) | E _x , MeV | J _f , | Exp. values | | Theory [13] | |
|---------------|-------------------------|------------------|------------------------------------|------------------------------------|---------------------------------|---------------------------------|
| | | | C ² (S _{3/2}) | C ² (S _{1/2}) | C ² S _{3/2} | C ² S _{1/2} |
| 387 keV | 0.00 | (3/2)- | 0.207 | 0.18 | 0.431 | 0.289 |
| | 0.429 | (1/2)- | 0.306 | 0.065 | 0.854 | 0.039 |
| 690 keV | 0.00 | (3/2)- | 0.357 | 0.208 | 0.431 | 0.289 |
| | 0.429 | (1/2)- | 0.729 | 0.056 | 0.854 | 0.039 |
| 984, 1283 keV | 0.00 | (3/2)- | 0.431 | 0.209 | 0.431 | 0.289 |
| | 0.429 | (1/2)- | 0.910 | 0.045 | 0.854 | 0.039 |

Another group of spectroscopic factors were extracted with only our OMPs and just changing in the spectroscopic factors to analysis the experimental data and this is shown as *solid line* in fig. 3. The spectroscopic factors of ${}^7\text{Be}$ at these low energies are energy dependent so their values changed with energy especially at very low energies. For example, the spectroscopic factors for ground state extracted were $1P_{3/2}=0.207$ and $1P_{1/2}=0.18$ and for excited state were $1P_{3/2}=0.306$ and $1P_{1/2}=0.065$ at $E_p=387$ keV. By increasing energy, the values of spectroscopic factors also have

been changed to analyze the experimental data as shown in table 2. The right values of spectroscopic factors depend on the choice of OMPs used.

In order to calculate the astrophysical S factor, we employed the standard expression [16]:

$$S(NJ, J_f) = \sigma(NJ, J_f) E_{\text{cm}} \exp\left(\frac{31.335 Z_1 Z_2 \sqrt{\mu}}{\sqrt{E_{\text{cm}}}}\right) \quad (3)$$

which was proposed as far back as the 1950s in [17] and where σ is the total cross section for the radiative capture process (in barn units), $E_{\text{c.m.}}$ is the c.m. energy of particles in the entrance channel (in keV units), μ is the reduced mass of the entrance-channel particles (in atomic mass units), Z are the charges of the particles (in elementary charge units, e) and N stands for E (electric) or M (magnetic) transitions of multipolarity J to the final (J_f) state of the nucleus. The numerical coefficient 31.335 was obtained by the present authors on the basis of modern values of fundamental constants from [18]. We have $S(0)=114\pm 5$ eV.b as shown in Figure.

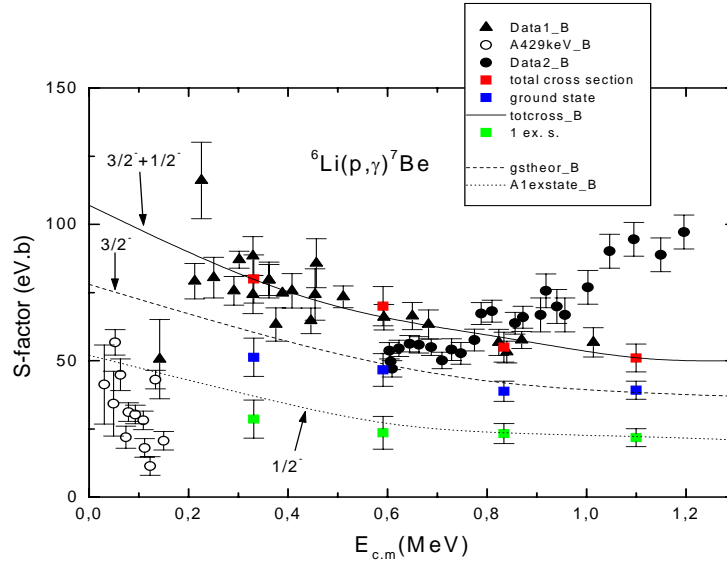


Fig. 4. S-factor calculated using our measurements and Fresco program, the red points are our measurements. The displayed points correspond to experimental data from [5] (they are presented in [7])

Second method of calculation of S-factor

The OMPs are widely employed to generate the distorted waves used to analyze the cross section of many reactions, and these analyses have proved to be a powerful tool to extract nuclear structure information. Reactions at astrophysical energies are complicated by the fact that the matter-interaction energy in stars is very low, ranging between a few tenths of a keV unit and a few tens of keV units. With a few exceptions, it is next to impossible under laboratory conditions to measure directly, at such energies, nuclear-reaction cross sections, which are necessary for astrophysical calculations. Usually, cross sections are measured at higher energies, whereupon the results are extrapolated to the energy region of interest for nuclear astrophysics. As a rule, however, the measurements actually performed cover only the region of rather high energies from about 0.2 to 1 MeV. In view of this, an extrapolation of such experimental data to the astrophysical region is not always justified. As a result, only theoretical predictions can compensate in many cases for missing experimental information about the properties of astrophysical thermonuclear reactions. Under such conditions, resort to realistic models that are rather simple in practical applications, such as the potential cluster model (PCM), seems quite justified. Usually, the results of calculations

performed on the basis of model concepts are contrasted against available low-energy experimental data, and approaches leading to the best agreement with these data are selected by using the results of this comparison. After that, calculations in the region of astrophysical energies are performed within the chosen conceptual framework. One can consider the results obtained in this way (for example, those concerning astrophysical S factors) as more realistic estimates of respective quantities than the extrapolation of experimental data, since the theoretical models used have, as a rule, quite a sound microscopic basis. Radiative capture of nucleons at energies of astrophysics interest is one of the most important processes for nucleosynthesis. The nucleon capture can occur either by a compound nucleus reaction or by direct process. The compound reaction cross sections are usually small, especially for light nuclei. The direct capture proceeds either via the formation of a single-particle resonance or non-resonant capture process.

To calculate the astrophysical S -factor, one must know the potentials of the inter-nuclear $p^6\text{Li}$ interaction in different states which can be constructed on the basis of elastic scattering phases resulting from phase shift analysis. Earlier, the phase shift analysis of the elastic $p^6\text{Li}$ scattering was performed for the energy range 0.5–5.6 MeV, taking into account spin-orbital phase splitting [19], however, no account was taken of the doublet 2P wave. The results of work [19] are shown in Fig. 4 by circles and open triangles, whereas our results taking into account the doublet 2P wave but without spin-orbital phase splitting – by dots and triangles. It is seen that the doublet 2S -phase obtained in [20] decreases much slower than it follows from analysis of work [19]. Thus, taking into account the doublet 2P wave [129] results in somewhat different 2S phases, and, hence, different potentials. In order to find the partial inter-cluster $p^6\text{Li}$ interactions using available scattering phases, use is made of an ordinary Gauss potential with a point Coulomb term, which can be written as follows [20]:

$$V(r) = -V_0 \exp(-\alpha r^2)$$

The following values are obtained for the parameters of potentials of the S -waves in two spin phase channels [19]:

$$^2S: V_0 = 110.0 \text{ MeV}, \alpha = 0.15 \text{ fm}^{-2},$$

$$^4S: V_0 = 190.0 \text{ MeV}, \alpha = 0.2 \text{ fm}^{-2}.$$

These potentials have two forbidden bound states (FS) each, with the latter corresponding to the Young diagrams $\{52\}$ and $\{7\}$ [21]. Figure 1 shows the results of calculations of the doublet 2S - and quartet 4S -phases of elastic scattering with these potentials by solid lines.

The astrophysical S factor was analyzed with allowance for the $E1$ transitions from the 2S - and 2D wave states of $p^6\text{Li}$ scattering to the $^2P_{3/2}$ ground and the $^2P_{1/2}$ first excited bound state of the ^7Be nucleus in the $p^6\text{Li}$ channel. The calculation of the wave function for the 2D scattering state without allowance for spin-orbit splitting was performed on the basis of the 2S -wave potential at $L = 2$.

In order to calculate the astrophysical S factor, we employed the standard expression [22]:

$$S(NJ, J_f) = \sigma(NJ, J_f) E_{\text{cm}} \exp\left(\frac{31.335 Z_1 Z_2 \sqrt{\mu}}{\sqrt{E_{\text{cm}}}}\right) \quad (4)$$

which was proposed as far back as the 1950s in [23] and where σ is the total cross section for the radiative capture process (in barn units), $E_{\text{c.m.}}$ is the c.m. energy of particles in the entrance channel (in keV units), μ is the reduced mass of the entrance-channel particles (in atomic mass units), Z are the charges of the particles (in elementary charge units, e) and N stands for E (electric) or M

(magnetic) transitions of multipolarity J to the final (J_f) state of the nucleus. The numerical coefficient 31.335 was obtained by the present authors on the basis of modern values of fundamental constants from [24].

In the above expression for the S factor, we isolated explicitly quickly changing exponential factor $P(E)$ generated by the Coulomb barrier. In response to the change in the energy, the S factor therefore changes much more slowly than the cross sections. The factorization of the cross section in the form:

$$\sigma(NJ, J_f) = S(NJ, J_f)P(E) \quad (5)$$

simplifies considerably the behavior of the S factor as a function of energy even in the resonance region. In the potential cluster model, the total radiative capture cross sections $\sigma(NJ, J_f)$ have the form (see, for example [25]):

$$\begin{aligned} \sigma_c(NJ, J_f) &= \frac{8\pi K e^2}{\hbar^2 q^3} \frac{\mu}{(2S_1 + 1)(2S_2 + 1)} \frac{J + 1}{J[(2J + 1)!!]^2} \times \\ &\times A_J^2(NJ, K) \sum_{L_i, J_i} P_J^2(NJ, J_f, J_i) I_J^2(J_f, J_i) \end{aligned} \quad (6)$$

where, for electric orbital [$EJ(L)$] transitions ($S_i = S_f = S$), we have

$$\begin{aligned} P_J^2(EJ, J_f, J_i) &= \delta_{S_i S_f} \left[(2J + 1)(2L_i + 1)(2J_i + 1)(2J_f + 1) \right] \times \\ &\times (L_i 0 J 0 | L_f 0)^2 \left\{ \begin{matrix} L_i & S & J_i \\ J_f & J & L_f \end{matrix} \right\}^2 \\ A_J(EJ, K) &= K^J \mu^J \left(\frac{Z_1}{m_1^{J_1}} + (-1)^J \frac{Z_2}{m_2^{J_2}} \right), \\ I_J(J_f, J_i) &= \langle \chi_f | R^J | \chi_i \rangle \end{aligned} \quad (7)$$

Here, q is the wave number of entrance-channel particles; L_f , L_i , J_f , and J_i are the particle angular momenta in the entrance (i) and exit (f) channels; S_1 and S_2 are particle spins; m_1 and m_2 (Z_1 and Z_2) are the masses (charges) of entrance-channel particles; K and J are, respectively, the wave number and the photon momentum in the exit channel; and I_J is the integral of the wave functions for the initial (χ_i) and final (χ_f) states (that is, the functions describing the relative motion of the clusters) with respect to the inter-cluster distance R . Sometimes, the spectroscopic factor S_{J_f} for the final state of the nucleus is included in the above expression for the cross sections but, in the potential cluster model used in this study, it is equal to unity.

The dashed curve in this figure represents the result for the transitions from the 2S and 2D scattering waves to the ground state of the ^7Be nucleus, the dotted curve represents the results for transitions to the first excited state, and the solid curve represents the total S factor. The displayed points (triangles and closed and open circles) stand for experimental data obtained in [5] (they are presented in [7]). The calculated $S_{1/2}$ factor (dotted curve) describes quite well experimental data for transitions to the first excited state of the ^7Be nucleus at low energies (open circles). The $S(10)$ factor at 10 keV is $S_{3/2} = 76$ eV b and $S_{1/2} = 38$ eV b, its total value being 114 eV b. For the sake of comparison, we present known results for the total $S(0)$ factor from various studies. They are 79(18)

[8], 105 (at 10 keV) [7], and 106 eV b [6]. The S -factor values presented in [9] are 39 eV b for transitions to the ground state and 26 eV b for the transition to the first excited state, so that the total S factor is 65 eV b. One can readily see that the scatter of these experimental data is rather large, and our results agree with them in general, see also our publication [26].

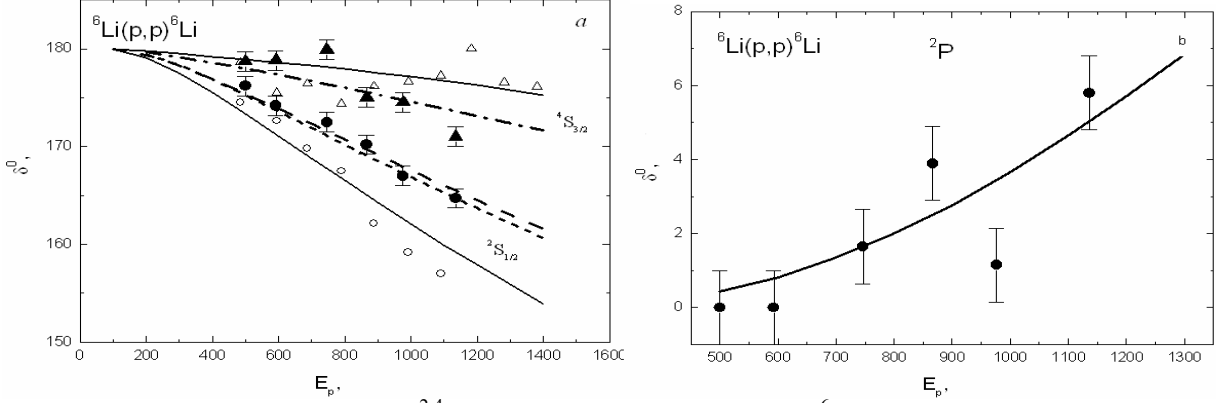


Fig. 5. (a) Doublet and quartet ${}^{2,4}S$ -wave phase shifts for elastic $p{}^6\text{Li}$ scattering at low energies in the presence of the 2P wave for the case where the 4P -wave phase shift is taken to be zero: (closed circles and triangles) results of our present analysis for, respectively, the 2S and 4S -wave phase shifts; (open circles and triangles) results of the partial-wave analysis performed in [19]; (curves) results of the calculations with various potentials (see main body of the text). (b) Doublet 2P -wave phase shifts for elastic $p{}^6\text{Li}$ scattering at low energies: (points) results of our present partial-wave analysis for the 2P -wave phase shifts at ${}^4P = 0$ and (curve) result of the calculations with the potential found in our study (see main body of the text), E_p in MeV and δ in degree

In Fig.6, the energy dependence of the total S factor calculated with the above potential is represented by the dash-dotted curve. Within the errors, this curve is compatible with experimental data at energies below 1 MeV.

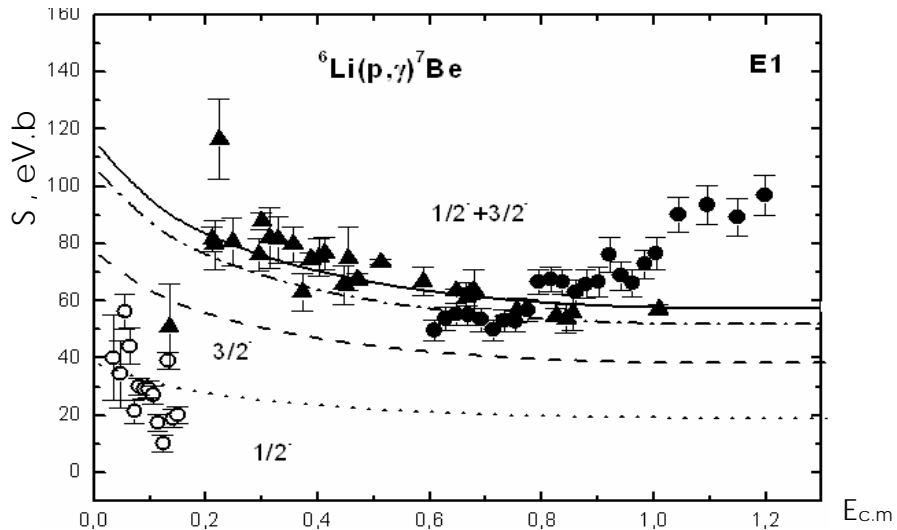


Fig. 6. Astrophysical S factor for the capture reaction $p{}^6\text{Li} \rightarrow {}^7\text{Be} \gamma$. The displayed points correspond to experimental data from [5] (they are presented in [7]). The dashed, dotted, solid, and dash-dotted curves represent, respectively, results for the transitions from the $2S$ and $2D$ scattering waves to the ground state of the ${}^7\text{Be}$ nucleus, results for transitions to the first excited state, the total S factor, and results of the calculations with a modified $2S$ -wave potential

Conclusion

The values of spectroscopic factors extracted in agree with theoretical calculation but at low energies still energy dependent. Astrophysical S-factor could be calculated using potential model and its value could be enhanced by enhancement of the OMPs used especially at low energies. In the second method, phase shift analysis could achieve the purpose, to extract S-factor in range of experimental data. So, both of them (methods used here) were proper to achieve and extract S-factor. ANC method also may be suitable to extract S-factor and this is our near future work.

References

1. N. Burtbayev, Mrarzhan Nasurralla, Maulan Nasurralla, Zh. K. Kerimkulov, and S. B. Sakuta, American institute of Physics (AIP) Conference Proceeding 2008, 203-208.
2. S. B. Dubovichenko; N. Burtebaev; D. M. Zazulin ; Zh. K. Kerimkulov; A. S. A. Amar, Physics of Atomic Nuclei, 2011, Volume 74, Number 7, Pages 984-1000.
3. J. T. Huang, C. A. Bertulani, V. Guimaraes, Atomic Data and Nuclear Data Tables 96(2010) 824-847.
4. S. Angulo et al., Nucl. Phys. A 656, 3 (1999).
5. Z. E. Switkowski, J. C. P. Heggie, D. L. Kennedy, D. G. Sargood, F. C. Barker, R. H. Spear, Nucl. Phys. A, Vol. 331 (1979) 50-60.
6. F. C. Barker, Aust. J. Phys. 33 (1980) 159.
7. K. Arai, D. Baye, P. Descouvemont, Nucl. Phys. A 699 (2002) 963-975.
8. R. M. Prior, M. C. Spraker, A. M. Amthor, K. J. Keeter, S. O. Nelson, A. Sabourov, K. Sabourov, A. Tonchev, M. Ahmed, J. H. Kelley, D. R. Tilley, H. R. Weller, and H. M. Hofmann, physical review C 70, 055801 (2004).
9. F. E. Cecil, D. Ferg, H. Liu, J. C. Scorby, J. A. McNeil, and P. D. Kunz, Nucl. Phys. A539, 75 (1992).
10. S. B. Dubovichinko, N. Burtebayev, D. M. Zazulin, Zh. K. Kerimkulov, A. Amar. Yad. Fizika, Vol. 74, No. 7, (2011) 1013-1028.
- A. Amar, Sh. Hamada, N. Burtebayev, N. Amangeldy, International Journal of Modern Physics E, Vol. 20, No. 4 (2011) 980-986.
11. J. D. King, R. E. Azuma, J. B. Vise, J. Görres, C. Rolfs, H. P. Trautvetter, A. E. Vlieks, Nucl. Phys. A, Vol. 567 (1994) 354-376.
12. S. Cohen and D. Kurath. Nucl. Phys. A101 (1967) 1.
13. R. Ostojic, K. Subotic, B. Stepanic // Nuovo Cim. A76, 1983, P. 73-82.
14. B. A. Watson, P. P. Singh, and R. E. Segel, Phys. Rev. Vol. 182, No. 4 (1969) 977-989.
15. W. A. Fowler, G. R. Caughlan, and B. A. Zimmerman, Ann. Rev. Astron. Astrophys. 13, 69 (1975).
16. E. E. Salpeter, Phys. Rev. 88, 547 (1952).
17. http://physics.nist.gov/cgi-bin/cuu/Value?hbar|search_for=universal_in!
18. C. Petitjean, L. Brown, and R. G. Seyler, Nucl. Phys. A 129, 209 (1969).
19. S. B. Dubovichenko and V. M. Zazulin, Russ. Phys. J., No. 5, 458 (2010).
20. S. B. Dubovichenko, The Properties of Light Atomic Nuclei within the Potential Cluster Model [in Russian], Daneker, Almaty, 2004.
21. W. A. Fowler, G. R. Caughlan, and B. A. Zimmerman, Ann. Rev. Astron. Astrophys. 13, 69 (1975).
22. E. E. Salpeter, Phys. Rev. 88, 547 (1952).
23. http://physics.nist.gov/cgi-bin/cuu/Value?hbar|search_for=universal_in!
24. S. B. Dubovichenko, The Methods for Calculation of Nuclear Characteristics [in Russian], Kompleks, Almaty, 2006.
25. S. B. Dubovichenko, N. Burtebaev, D. M. Zazulin, and A. S. A. Amar, Astrophysical s-factor of radiative $p^6\text{Li}$ capture at low energies, Russian Physics Journal, Vol. 53, No. 7, 2010.

ӘРТҮРЛІ ӘДІСТЕР АРҚЫЛЫ ЭКСПЕРИМЕНТТІК ДЕРЕКТЕРДЕН АЛЫНҒАН ${}^6\text{Li}(p,\gamma){}^7\text{Be}$ РЕАКЦИЯСЫНЫҢ АСТРОФИЗИКАЛЫҚ S-ФАКТОРЫ

Н. Бүртебаев, А. Амар, С.Б. Дубовиченко, С.Б. Сакута, С.В. Артемов, Ж. Керімкулов

${}^7\text{Be}$ негізгі және бірінші қозбалы күйлеріне ($1/2^-$, 429 кэВ) γ - өтулерінің $E_{p,\text{лаб}} = 387, 690, 984$ және 1283 кэВ сәуле энергияларында ${}^6\text{Li}(p, \gamma){}^7\text{Be}$ реакциясының бұрыштық үлестірілуінің жаңа өлшеулері орындалды. ${}^6\text{Li}(p, \gamma){}^7\text{Be}$ реакциясының қималарын есептеу Fresco программасын арқылы потенциалдық моделде тікелей қармау шеңберінде өткізілді. Эксперименттік деректерден ${}^7\text{Be}$ -дің спектроскоптық факторлары мен ${}^6\text{Li} + p \rightarrow {}^7\text{Be} + \gamma$ астро S-факторын екі әдісті қолдану арқылы алынды.

АСТРОФИЗИЧЕСКИЙ S-ФАКТОР РЕАКЦИИ ${}^6\text{Li}(p,\gamma){}^7\text{Be}$, ПОЛУЧЕННЫЙ ИЗ ЭКСПЕРИМЕНТАЛЬНЫХ ДАННЫХ С ИСПОЛЬЗОВАНИЕМ РАЗЛИЧНЫХ МЕТОДОВ

Н. Бүртебаев, А. Амар, С.Б. Дубовиченко, С.Б. Сакута, С.В. Артемов, Ж. Керимкулов

Новые измерения угловых распределений реакции ${}^6\text{Li}(p, \gamma){}^7\text{Be}$ были сделаны при энергиях $E_{p,\text{лаб}} = 387, 690, 984$ и 1283 кэВ γ - переходов в основное и первое возбужденное состояние ($1/2^-$, 429 кэВ) в ${}^7\text{Be}$. Расчеты сечения ${}^6\text{Li}(p, \gamma){}^7\text{Be}$ реакции проводили в рамках прямого захвата в потенциальной модели с использованием программы Fresco. Мы извлекли спектроскопические факторы ${}^7\text{Be}$ и астрофизический S-фактор ${}^6\text{Li} + p \rightarrow {}^7\text{Be} + \gamma$ из экспериментальных данных с использованием двух различных методов.